

CHAPTER IV

RESULTS AND DISCUSSION

4.1 Rheological behavior

4.1.1 Neat components and uncompatibilized binary blends

The plots of viscosity versus shear rate for the neat components and the blends were measured at temperature 250 °C and at shear rate range from 30 to 3200 s⁻¹, which are presented in figures.

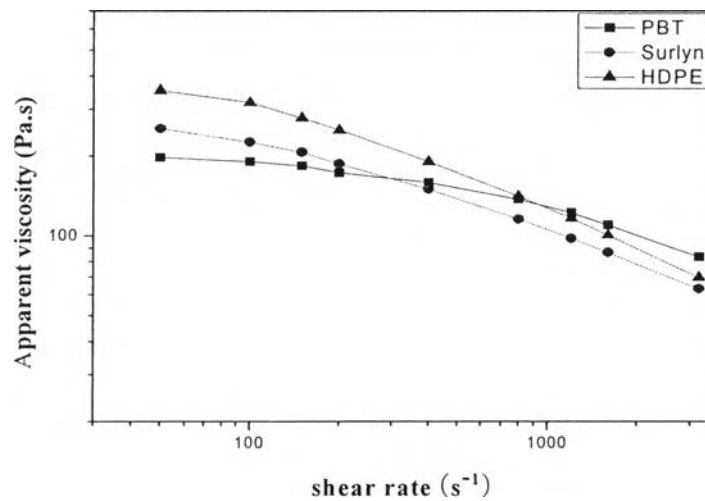


Figure 4.1 Flow curves of neat components.

Apparently, the neat PBT shows relatively low viscosity at lower shear rate region and less shear thinning at higher shear rate while neat HDPE has the highest viscosity. In addition, the viscosity of the Surlyn is higher than PBT, at least in the low shear rate region and the flow curve of HDPE is higher than Surlyn in the whole shear rate region.

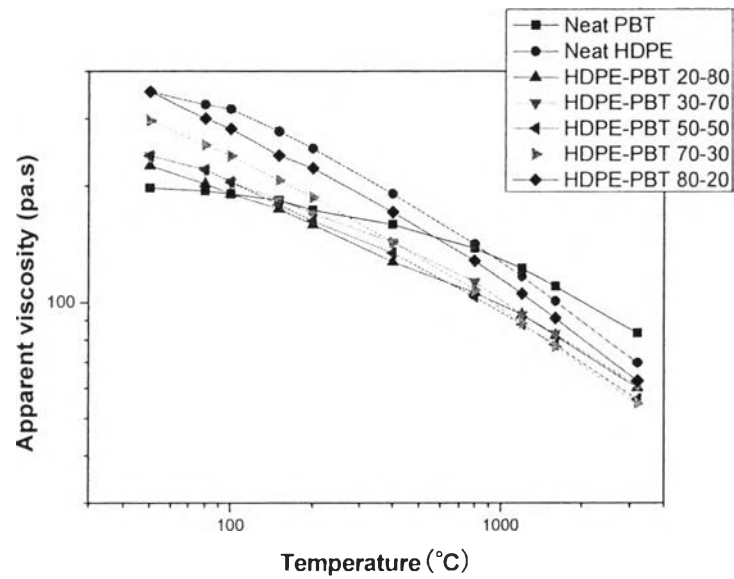


Figure 4.2 Flow curves of uncompatibilized binary blends and neat polymers.

All specimens exhibit shear-thinning behavior which interpreted as the viscosity decreases with increasing shear rate due to the induced chain orientation, resulting in a lower entanglement density. Noticing that molten PBT behaved like a Newtonian fluid at low shear rates and like a shear thinning fluid at high shear rate (i.e., greater than 800 s^{-1}). The shear viscosities for blend samples were found to increase with increasing HDPE content, and the values were found to locate between those of the two neat polymers.

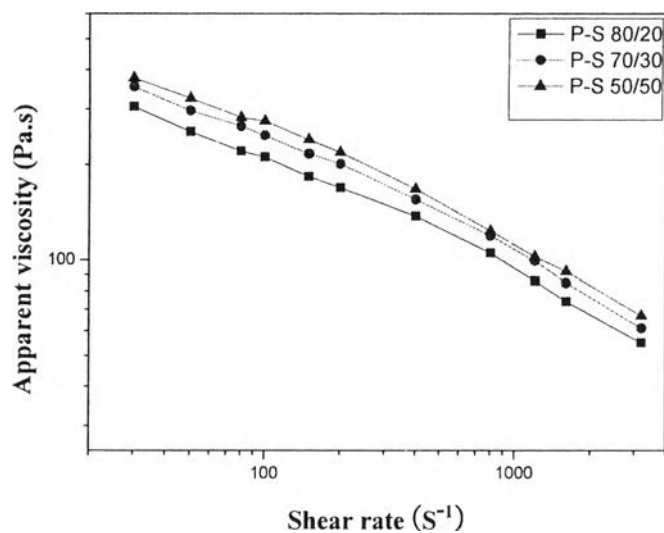


Figure 4.3 Flow curves of PBT/Suryln blends.

In Fig.4.3 the PBT/Suryln blends at ratio of 80/20, 70/30, 50/50, display greater shear thinning over the whole shear rate range than the neat PBT, indicating that introducing Suryln into the system could enhance its shear-thinning behavior. It is important to note that viscosity increase with increasing Suryln content, which indicate the compatibilizing reaction between PBT and Suryln has increased their interfacial adhesion.

4.1.2 Compatibilized ternary blends

The flow curves of ternary blends compatibilized with Na-EMAA (0, 1, 2.5, 5, 10 phr) at various compositions were plotted. In order to make comparison, the uncompatibilized binary blend was also plotted in the same figure.

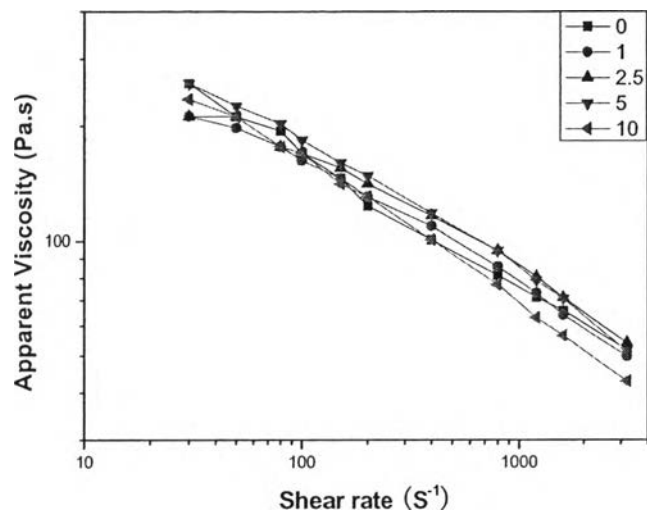


Figure 4.4 Flow curves of PBT/HDPE 80/20 blend containing various Surlyn contents of 0, 1, 2.5, 5, 10 phr.

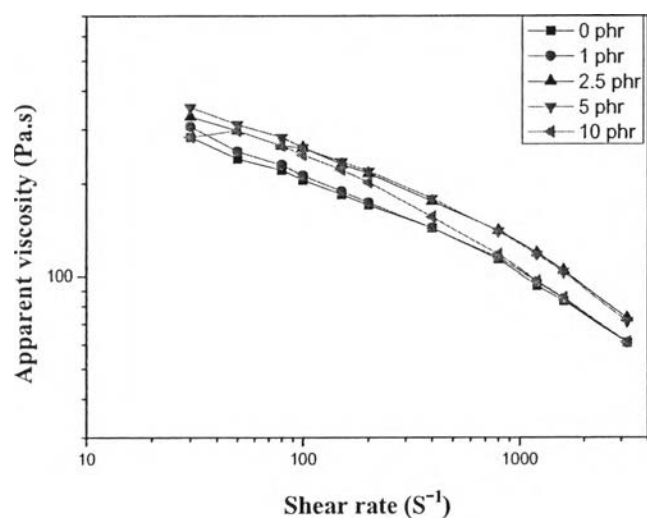


Figure 4.5 Flow curves of PBT/HDPE 70/30 blend containing various Surlyn contents of 0, 1, 2.5, 5, 10 phr.

In PBT-rich blends, using Surlyn to compatibilize the blends can enhance the viscosity, it seems to be highest viscosity when 5 phr of Surlyn used. Especially, the curve showed more shear thinning and the viscosity turn to decrease when the content of Surlyn increased to 10 phr. Fig.4.5, it showed 1phr Na-EMAA had small effect on viscosity, then viscosity increased obviously when 2.5 phr and 5 phr Na-EMAA were added.

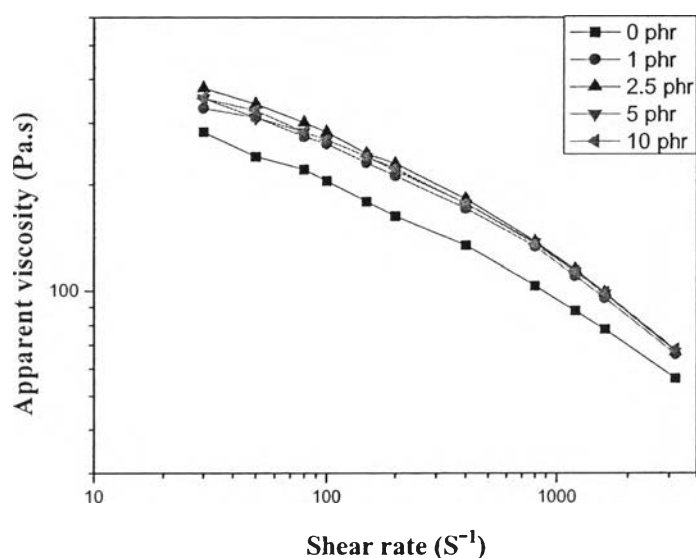


Figure 4.6 Flow curves of PBT/HDPE 50/50 blend containing various Surlyn contents of 0, 1, 2.5, 5, 10 phr.

In Fig.4.6. The flow curves of all the ternary compatibilized blends are similar and much higher than that of the binary blend. This drastically increasing can be due to the addition of a higher viscosity Na-EMAA component or to some compatibilizing action of the Na-EMAA both with HDPE and PBT.

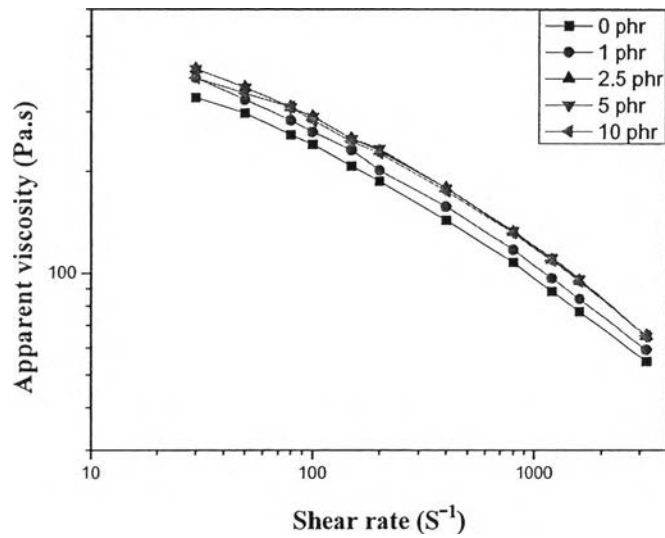


Figure 4.7 Flow curves of PBT/HDPE 30/70 blend containing various Surlyn contents of 0, 1, 2.5, 5, 10 phr.

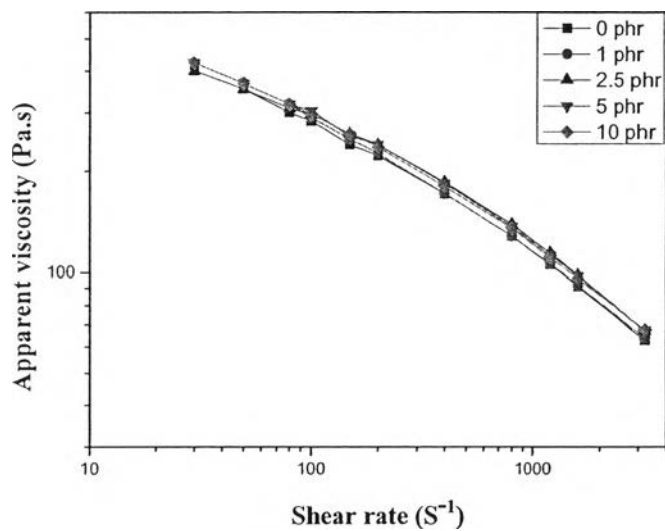


Figure 4.8 Flow curves of PBT/HDPE 20/80 blend containing various Surlyn contents of 0, 1, 2.5, 5, 10 phr.

In HDPE-rich blends, the viscosity increase with increasing the amount of Na-EMAA. Fig. 4.7 displays the viscosities of different content of Na-EMAA blends were slightly different after further addition of more than 1 phr, and it hard to distinct which one is the highest viscosity compared with 2.5 and 5 phr, but it can be seen 10 phr of Na-EMAA resulting a little decreasing of viscosity. However, in Fig.4.8, after using Na-EMAA, viscosity shows slightly variation and the location of flow curves of all blends are very close to each other, due to the highest viscosity of HDPE main phase compared with small amount of dispersed Na-EMAA and PBT minor phase.

4.2 Dynamic properties

4.2.1 The DMA results of $\tan \delta$ as a function of temperature were shown as below.

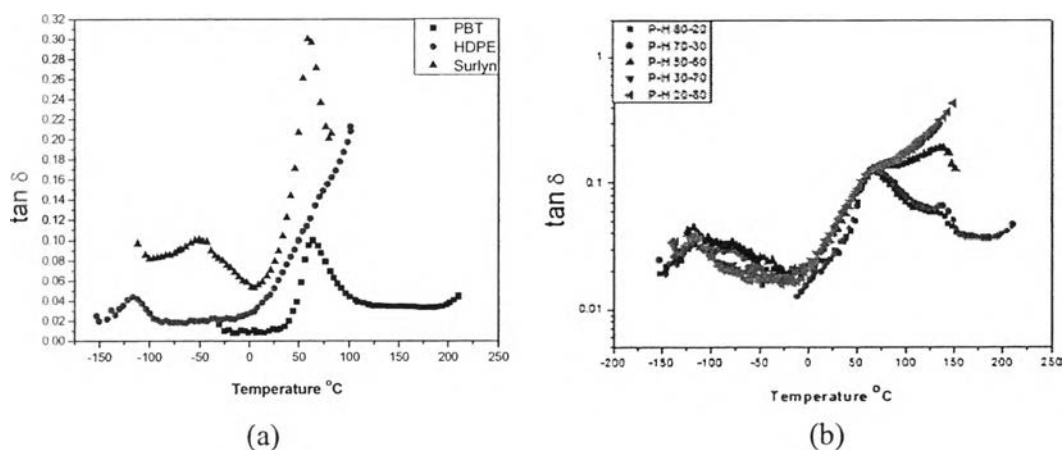
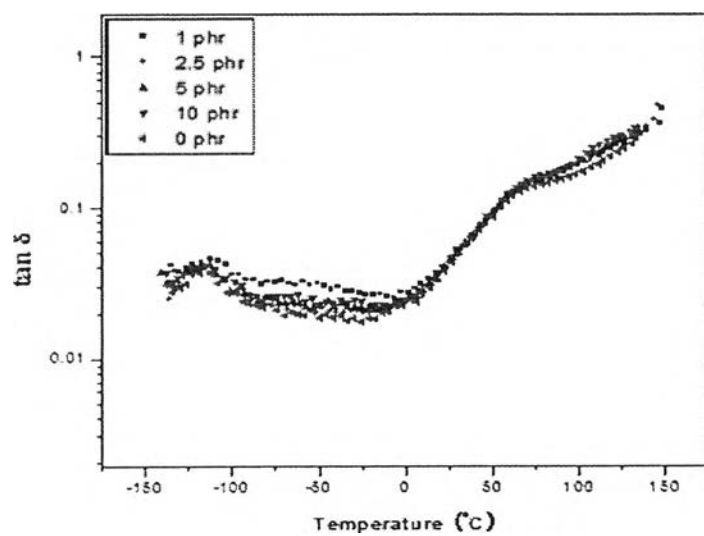


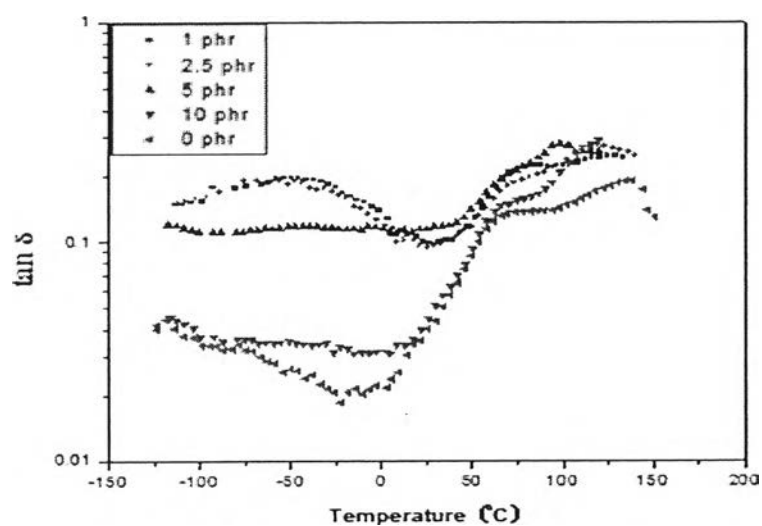
Figure 4.9 $\tan \delta$ as a function of temperature of neat compositions (a) and PBT/HDPE blends (b).

The occurrence of glass transitions can be clearly seen in the typical profiles of $\tan \delta$ versus temperature shown from Fig.4.9. The $\tan \delta$ peak of HDPE glass transition temperature is -116.3 °C, the $\tan \delta$ peak of PBT glass transition temperature is 64.1 °C, two $\tan \delta$ peaks of Surlyn is -50.7 and 58.9 °C respectively. In PBT/HDPE

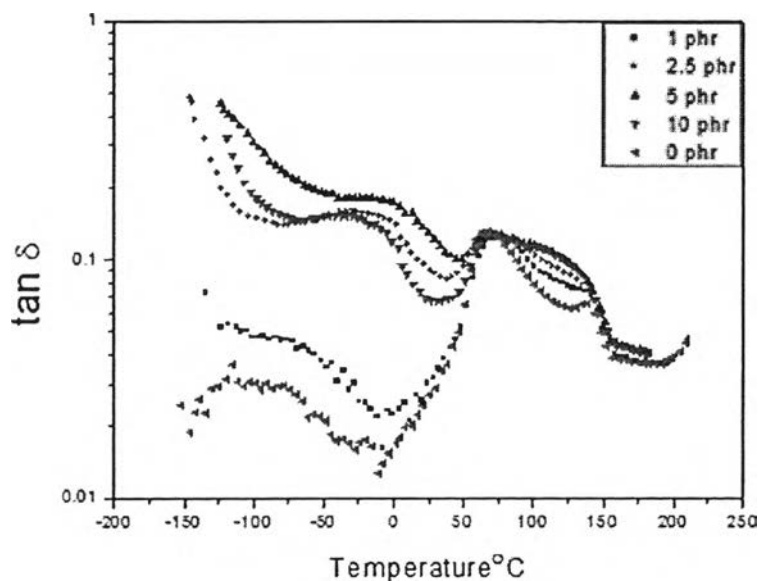
blends without compatibilizer, Fig.4.9 (b) two separate Tgs were observed, indicating that the blends were phase separated in the amorphous phase.



(a)



(b)

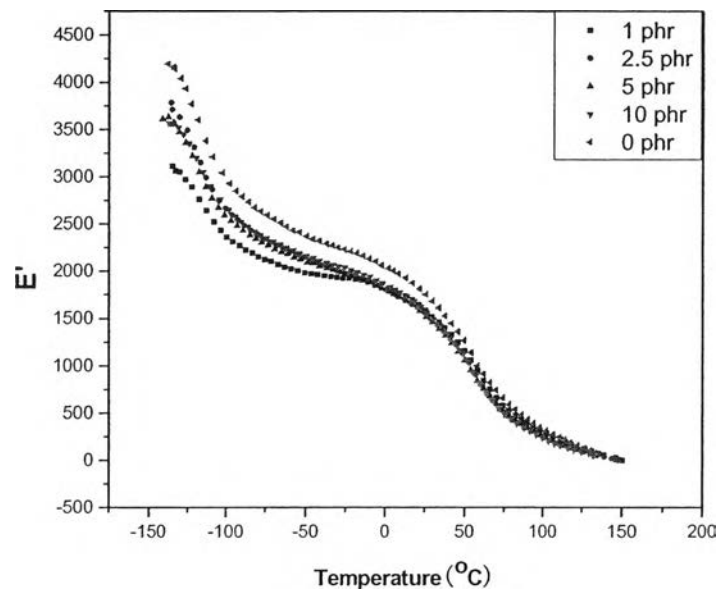


(c)

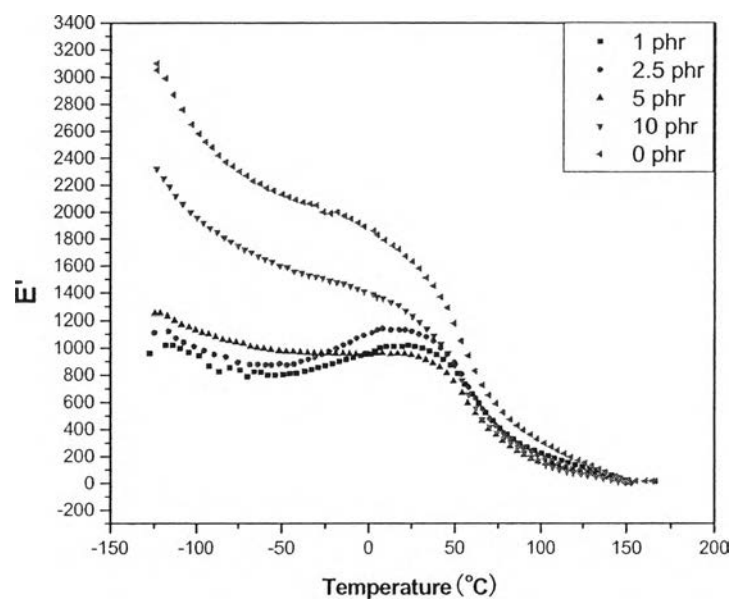
Figure 4.10 Tan δ as a function of temperature of different ratios of blends: PBT/HDPE 30/70 (a), PBT/HDPE 50/50 (b), PBT/HDPE 70/30 (c).

In PBT/HDPE/Surlyn ternary blends, the glass transition of these blends had changed. In Fig.4.10 (c), PBT/HDPE 70/30 blends showed that T_gs shifted close to each other after adding compatibilizer. It suggests that PBT and HDPE were more compatible after adding compatibilizer. In PBT/HDPE 30/70, blends show that a single T_g was observed in glass transition of HDPE, but the tan δ peak of glass transition of PBT minor phase became smooth. The curves were located closely, it seems like the compatibilizer has a little effect on compatibility. In PBT/HDPE 50/50, there were tangent peaks became flat after adding compatibilizer, indicating the improvement of compatibility.

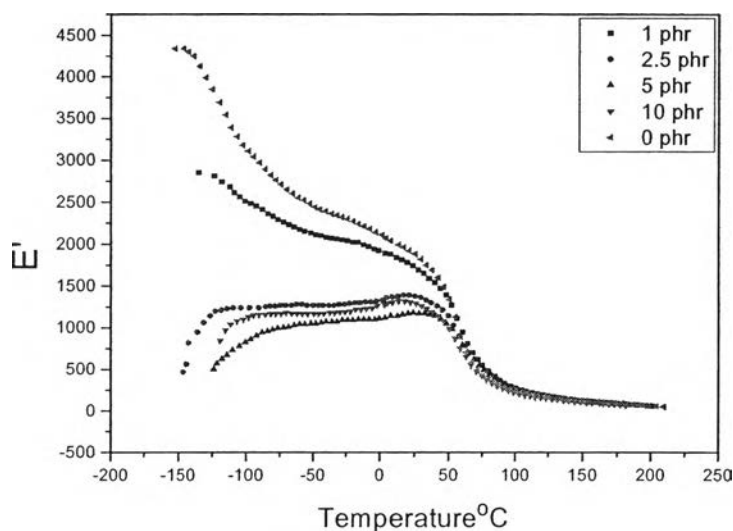
4.2.2 The DMA results of storage modulus as a function of temperature of PBT/HDPE blends with different amount of Surlyn as shown in figures.



(a)



(b)



(c)

Figure 4.11 Storage modulus E' as a function of temperature of different ratios of blends: PBT/HDPE 30/70 (a), PBT/HDPE 50/50 (b), PBT/HDPE 70/30 (c).

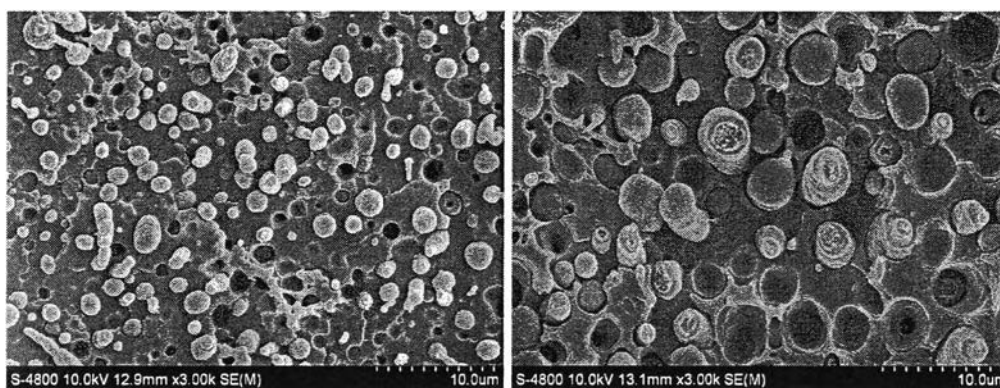
Typical DMA curves recorded for different ratio of components are displayed in Fig.4.11. In PBT/HDPE 30/70 with 0 phr Na-EMAA, the main features for the elastic modulus E' are: two sharp drops at the α transition, refer to HDPE and PBT respectively, a rubber plateau interrupted between these two temperatures. The variations in storage modulus E' show specimens which added Na-EMAA decreasing the storage modulus E' . 1phr of Na-EMAA blend has the lowest E' while 2.5, 5 and 10phr of specimens show the values closely.

In PBT/HDPE 50/50 and PBT/HDPE 70/30, from Fig. 4.11 (b) it showed a decreasing trend in storage modulus with increase in temperature. It can be seen that the variation of storage modulus with temperature seemed to be affected by the amount of Na-EMAA. With increasing content of Na-EMAA, the storage modulus E' turn to decrease, but 10phr of Na-EMAA showed higher storage modulus than 5phr of Na-EMAA due to the cross-link effect of Na-EMAA ionomer. In Fig. 4.11 (c) it still can be seen two drops at the α transition when 1 phr Na-EMAA added, but only one drop at the

α transition of PBT can be seen when further amount of Na-EMAA added (i.e., 2.5 phr, 5 phr and 10 phr). That indicate the compatibilization between PBT and HDPE has increased.

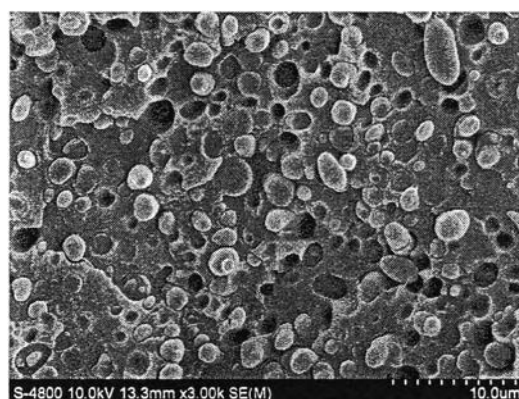
4.3 SEM morphology

The ultimate goal of compatibilization is to achieve stable phase morphology and improved mechanical performance. Mechanical properties of a heterogeneous polymer blend are directly related to its microstructure, especially the size and shape of the dispersed phase. Figures 4.12–4.16 show the SEM micrographs of the uncompatibilized and compatibilized by Surlyn for blends, respectively.



(a) HDPE/PBT 20/80

(b) HDPE/PBT 30/70



(c) HDPE/PBT 50/50

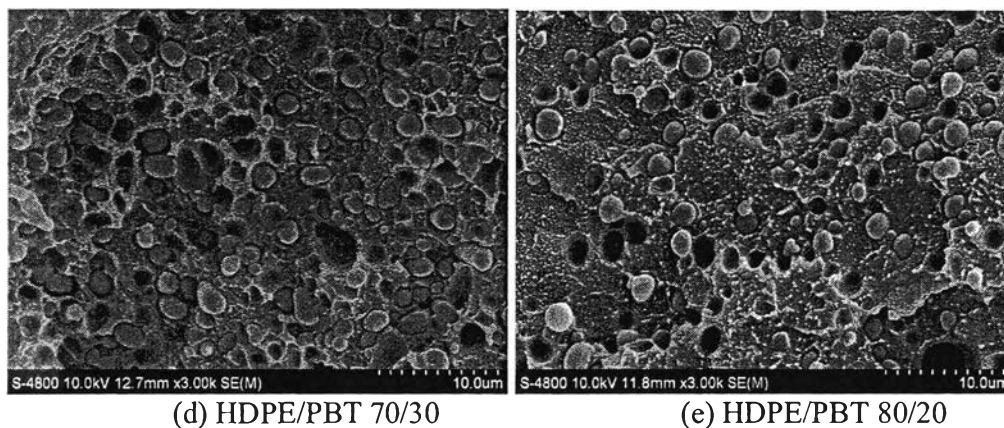


Figure 4.12 The SEM micrographs of the uncompatibilized HDPE/PBT blends at different ratio as (a) 20/80; (b) 30/70; (c) 50/50; (d) 70/30; (e) 80/20 respectively.

This set of micrographs show HDPE/PBT blends without compatibilizer, all of them show the incompatibility and their coarse phase exhibited big size of domain droplets. Noticing, at different ratios of PBT-rich phase, Fig.4.12 (b) showed bigger droplet size than Fig.4.12 (a), due to the different amount of HDPE content, as mentioned previously, HDPE has higher viscosity than PBT, when increase HDPE content, the droplet is more harder to break up. At different ratios of HDPE-rich phase, Fig.4.12 (d) showed that droplets were become much more crowd than Fig.4.12 (e) may due to the PBT molecular structure has much more resilience, so it is hard to disperse.

The liquid nitrogen fractured samples after etching by toluene which produced the representative SEM micrographs are shown in Fig.4.13. HDPE/PBT 80/20 with 1 phr Na-EMAA etched by hot toluene in order to remove HDPE phase. Micrographs were made a comparison to show the PBT droplets clearly, the dispersed PBT phase appeared as spherical domains.

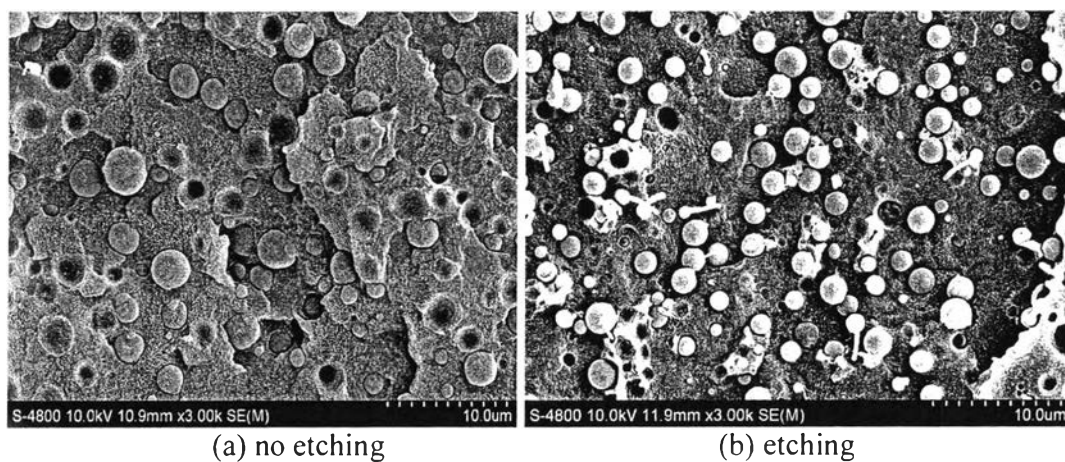


Figure 4.13 The SEM micrographs of HDPE/PBT 80/20 with 1 phr of Na-EMAA.

SEM micrographs of samples after cryogenic fracture of HDPE/PBT 30/70 with different amount of compatibilizer are shown in figures below.

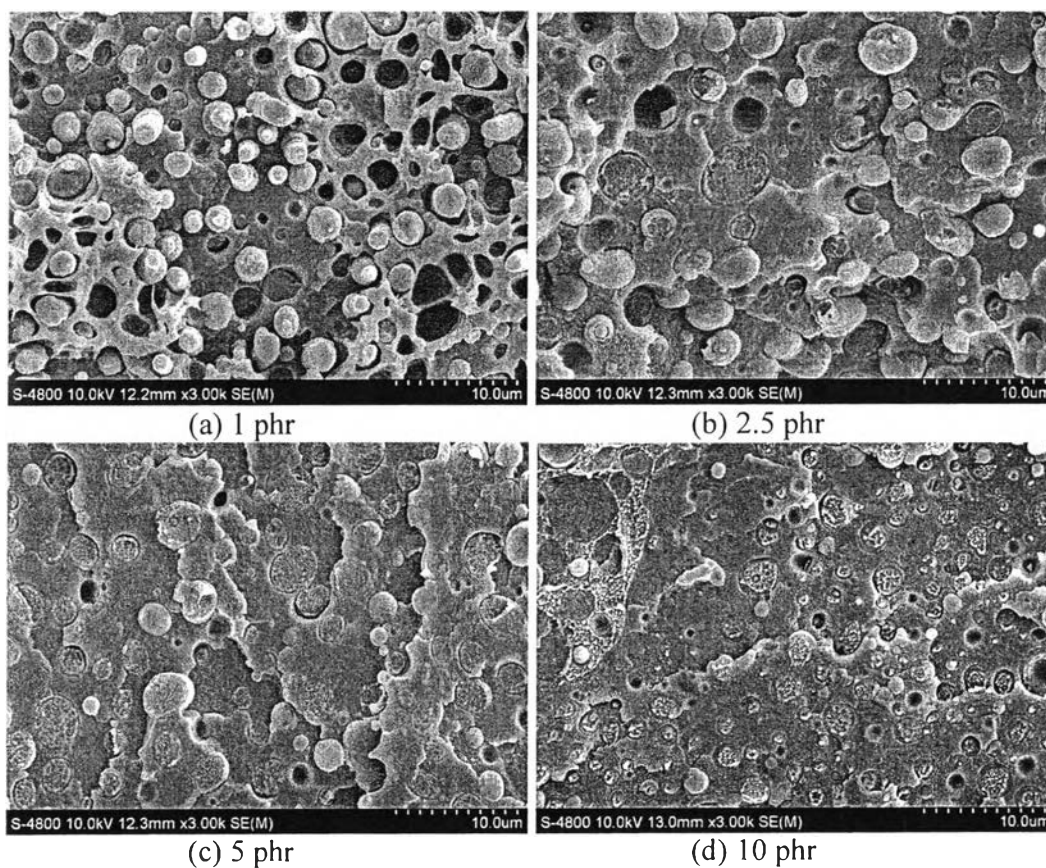


Figure 4.14 SEM micrographs of fractured surfaces of HDPE/PBT 30/70 with different amount of Na-EMAA.

These figures show apparent decreases in the domain size of the HDPE dispersed phases with adding different contents of Surlyn. There is no apparently further decrease in the domain size of the HDPE phase in the PBT-rich blends with a 5 phr of Surlyn content. The SEM micrographs showed the improvement of adhesion of interface, which can be associated with the result of mechanical properties would be discussed later.

SEM micrographs of samples after cryogenic fracture of HDPE/PBT 50/50 with different amount of compatibilizer are shown in figures below.

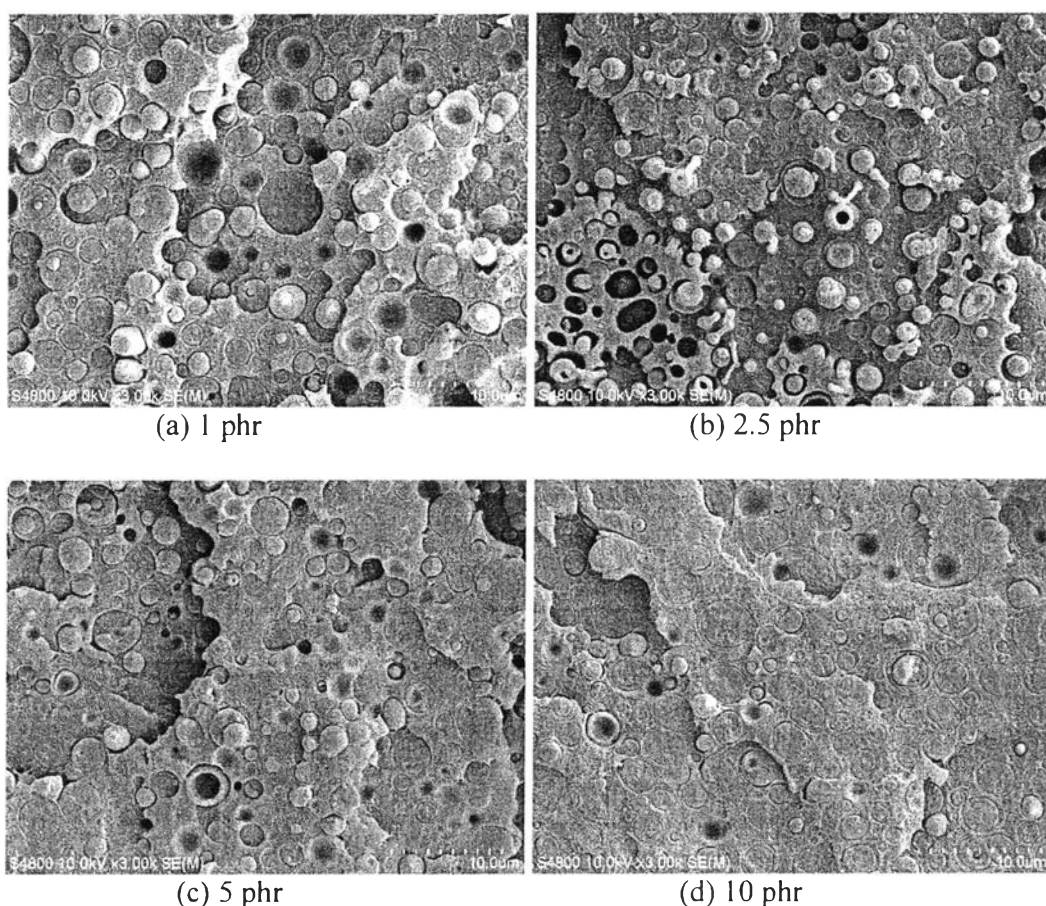


Figure 4.15 SEM micrographs of fractured surfaces of HDPE/PBT 50/50 with different amount of Na-EMAA.

The SEM of cryogenic fractures produced expected contrast between these two phases, and showed a more adhesive interfacial phase when added more than

2.5 phr of Na-EMAA, the particles was less polydisperse. The compatibility of these blends is attributed to the ethylene segments of Na-EMAA compatible to the HDPE and the Na-EMAA carboxylic acid reacts with the hydroxyl end groups of PBT. Due to the ionomer is only partly neutralized with sodium ion, additional carboxylic acids are available. It also worth noticing the physical interaction between PBT and ionomer can not be withdrawn. There are possible ways such as hydrogen bonding, ion-dipole interaction.

SEM micrographs of samples after cryogenic fracture of HDPE/PBT 70/30 with different amount of compatibilizer, are shown in figures below

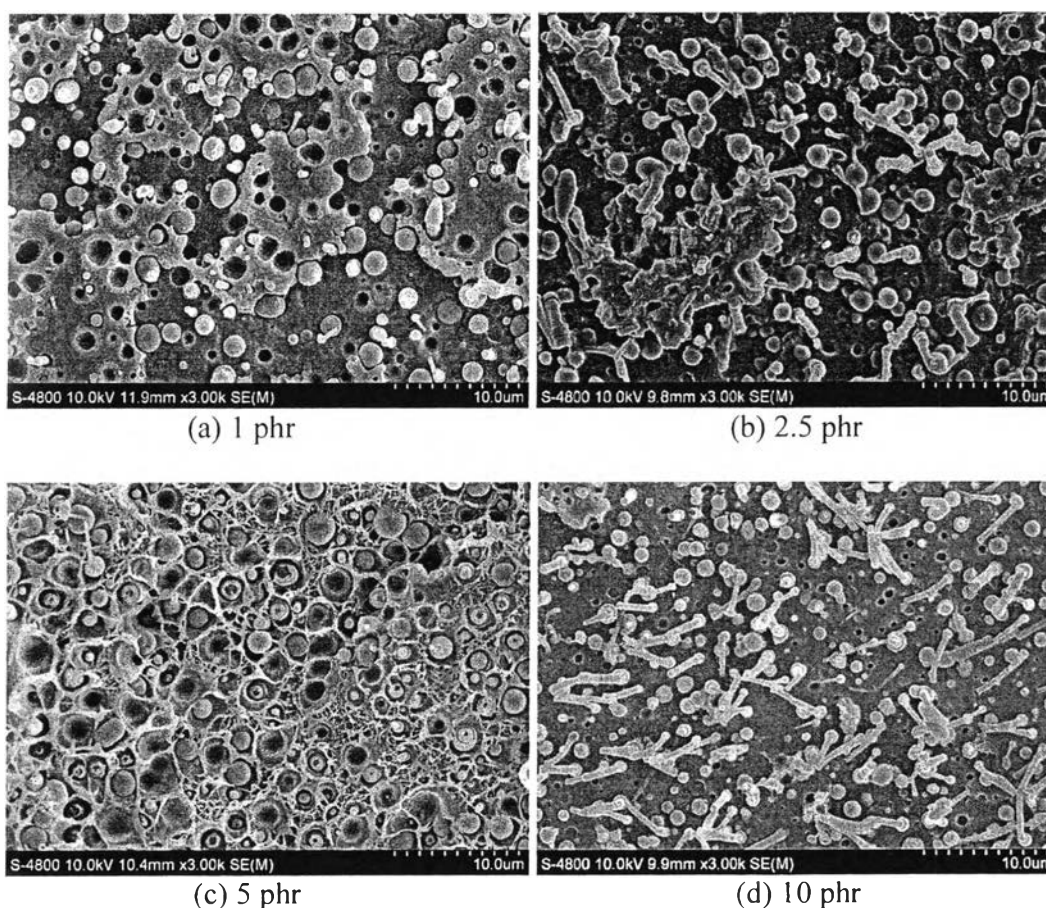


Figure 4.16 SEM micrographs of fractured surfaces of HDPE/PBT 70/30 with different amount of Na-EMAA.

The stability of dispersed phase domains of HDPE-rich blend was inserted by a series of pictures. The dispersed PBT phase formed as fibrillar and spherical domains, and the fibrillar domains become longer and more concentrated with increasing Na-EMAA content due to the phase coalescence. It is also found that the size of the dispersed droplets decrease drastically at addition of 10 phr compatibilizer. This reduction may be due to the improvement of the interfacial adhesion by compatibilizer forming an interphase.

Table 4.1 Number average diameter (μm) of dispersed phase size of blends

Surlyn	HDPE/PBT				
	20/80	30/70	50/50	70/30	80/20
0 phr	3.63	3.67	2.55	2.41	2.16
1 phr	3.54	1.83	2.20	1.60	2.03
2.5 phr	2.03	2.22	1.47	1.75	1.97
5 phr	2.10	1.83	1.48	1.67	1.85
10 phr	2.22	1.41	1.54	1.44	1.30

The number average diameters ranged between 1 and 4 μm and are shown in Table 4.1. The uncompatibilized blends demonstrated the biggest diameter of dispersed phase size over the whole range. All compatibilized blends displayed much smaller diameter. The compatibilizer is able to produce not only much finer morphology, but also to reduce the dispersed phase sizes.

4.4 Mechanical properties

4.4.1 Impact strength

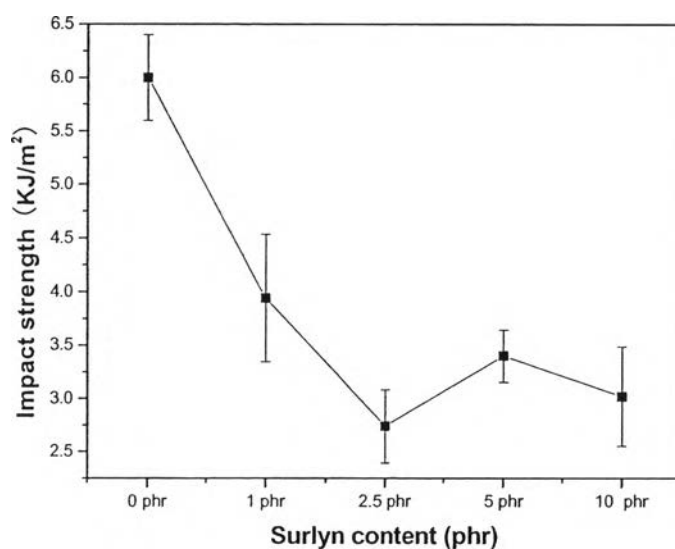


Figure 4.17 Variation of impact strength with Surlyn content in the blend of PBT/HDPE 70/30.

In Fig.4.17 the impact strength of uncompatibilized blend can be considered the highest. An enhancement of impact strength was observed in blends containing 5 phr Surlyn compared with 2.5 phr of it. Due to the compatibilized action hold the two phases together at higher loading by extending themselves. Lower impact strength at 10 phr surlyn was due to the presence of higher amount of shorter molecules of Surlyn, which plasticized the phase, thereby weakened the inherent strength of the components.

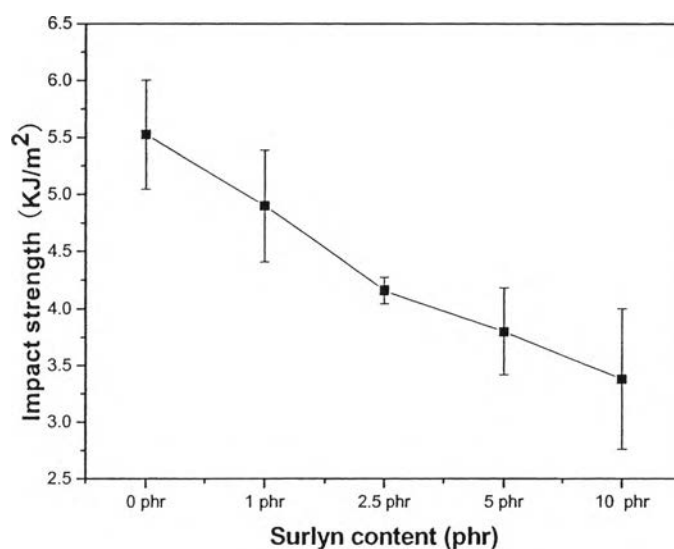


Figure 4.18 Variation of impact strength with Surlyn content in the blend of PBT/HDPE 50/50.

The impact strength of PBT/HDPE 50/50 blend was shown in Figure 4.18. There is a distinct decreasing trend of impact strength from uncompatibilized blend to compatibilized blend until compatibilizer content increased to 10 phr.

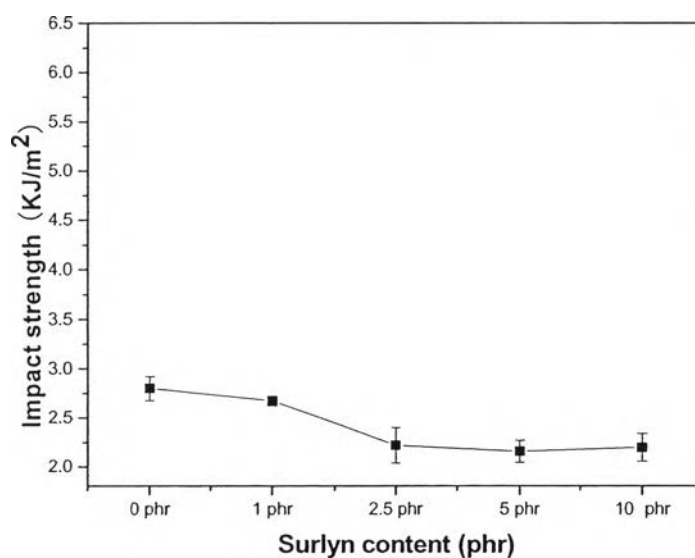
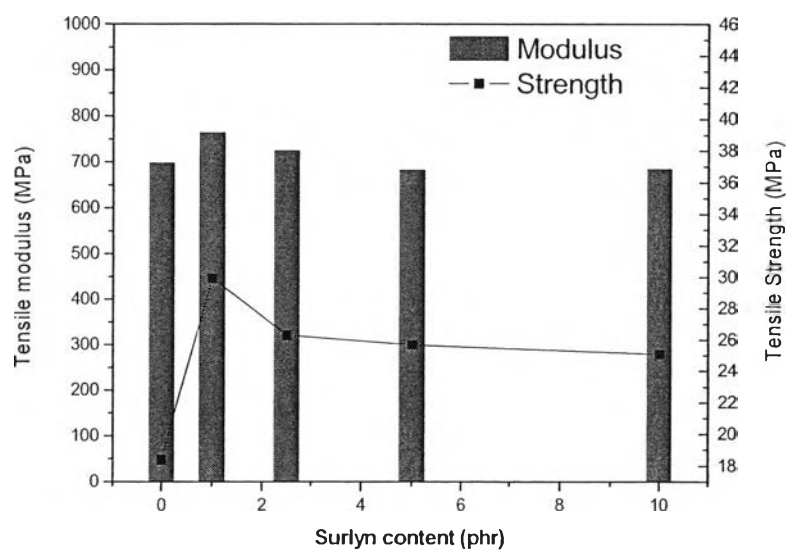


Figure 4.19 Variation of impact strength with Surlyn content in the blend of PBT/HDPE 30/70.

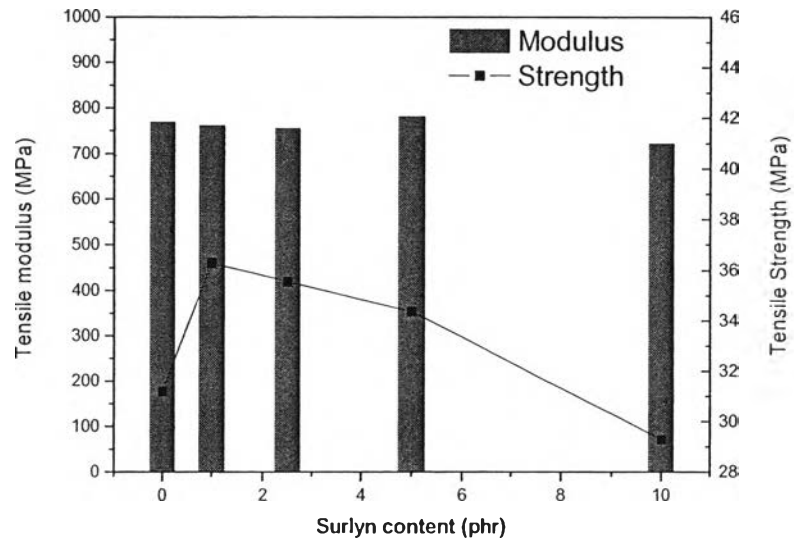
The impact strength of PBT/HDPE 30/70 blend was shown in Figure 4.19. The impact strength of this blend displayed much smaller values than other two ratios of blends, and it showed a slightly decreasing trend until the compatibilizer content increased to 2.5 phr, then further amount of compatibilizer didn't change the impact strength too much.

4.4.2 Tensile properties

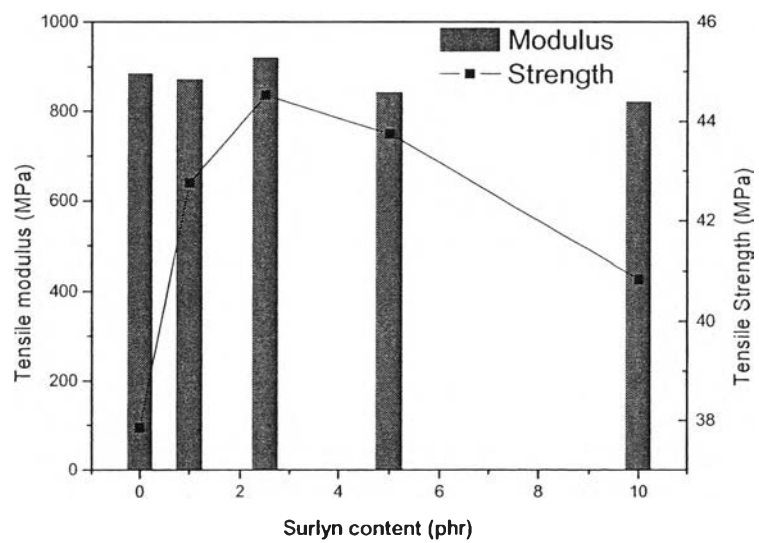
The tensile properties of PBT/HDPE blends with different content of Surlyn are shown as below.



(a)



(b)



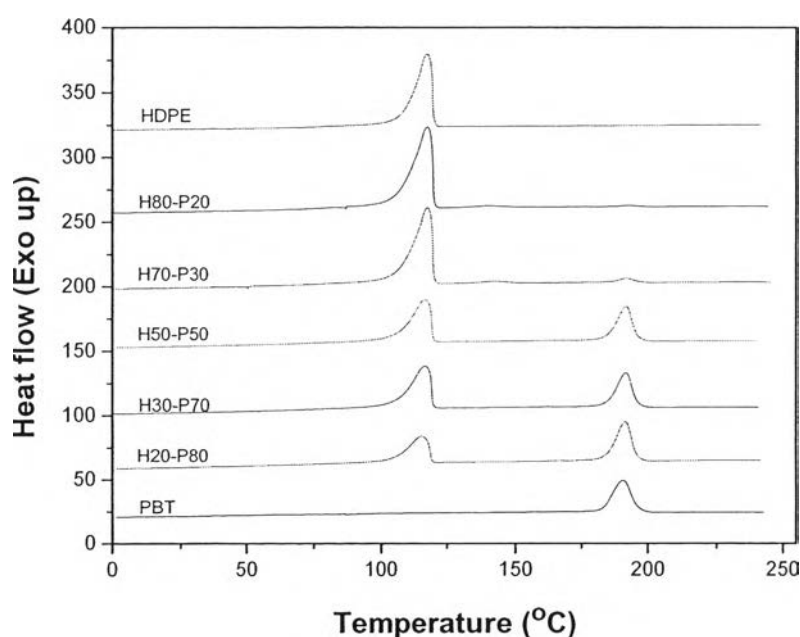
(c)

Figure 4.20 Variation of tensile strength and tensile modulus with Surlyn content in the blend of HDPE/PBT 70/30 (a), HDPE/PBT 50/50 (b), and HDPE/PBT 30/70 (c).

It is reported that the tensile properties of polymer blends are very sensitive to the state of the interface, that is, interfacial adhesion. As mentioned above, the reactions could happen between PBT and Surlyn, On the other hand, the SEM micrographs showed the improvement of fractured surface after using compatibilizer. So, the apparently improvement in the tensile strength of the blends is believed to be related to the improved interfacial adhesion between the PBT and HDPE. It is seen that the tensile modulus has a little variation with increasing Surlyn content, but the tensile strength are maximum improved by the introduction of 1 phr of Surlyn at ratios of HDPE/PBT 70/30 and HDPE/PBT 50/50, except HDPE/PBT 30/70 is maximum improved by 2.5 phr of Surlyn. To compare these blends, higher content of PBT displayed the higher tensile strength and modulus.

4.5 Thermal property

DSC thermograms for HDPE, PBT, and HDPE/PBT blend samples recorded during cooling and heating traces at a rate of 10 °C/min are both presented in Figure 4.21.



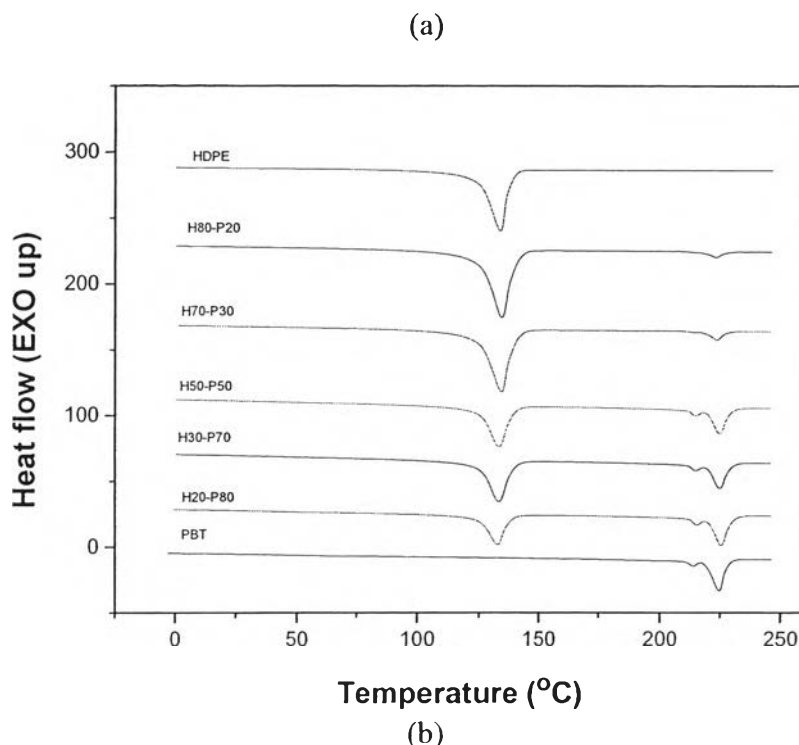


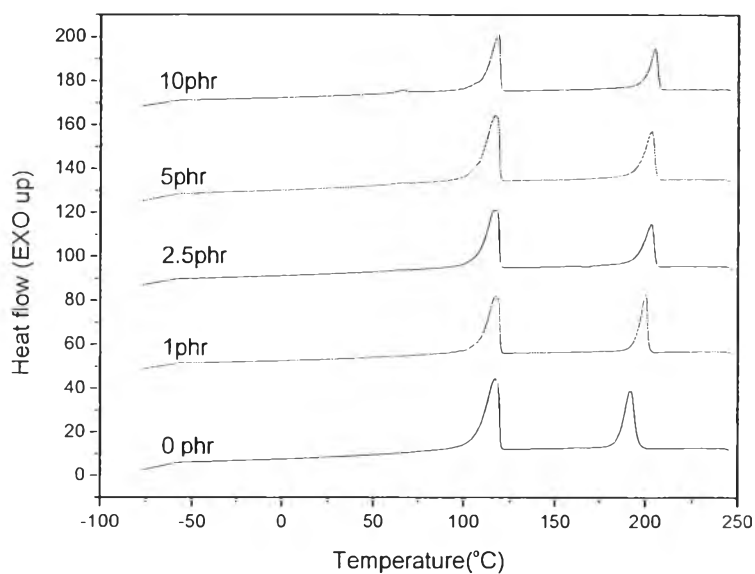
Figure 4.21 DSC melt crystallization exotherms (a) and melting thermograms (b) for HDPE, PBT, and HDPE/PBT blend samples recorded during cooling and heating at 10 °C/min.

In Fig.4.21 (a) The cooling trace suggested that both HDPE and PBT components in the blends crystallized concurrently, the area of exothermal peaks identify HDPE molecules were more crystallizable, while PBT molecules were less crystallizable. When the HDPE content was more than 70 percent, the peak area of PBT is obviously smaller than that of HDPE. However, the melt crystallization temperature (peak temperature) of each phase of the blends didn't change too much. As it is known, the crystallinity is dependent on the molecular structure of the polymer chains. HDPE has lower content of short branched-chain segments that promote the crystallization.

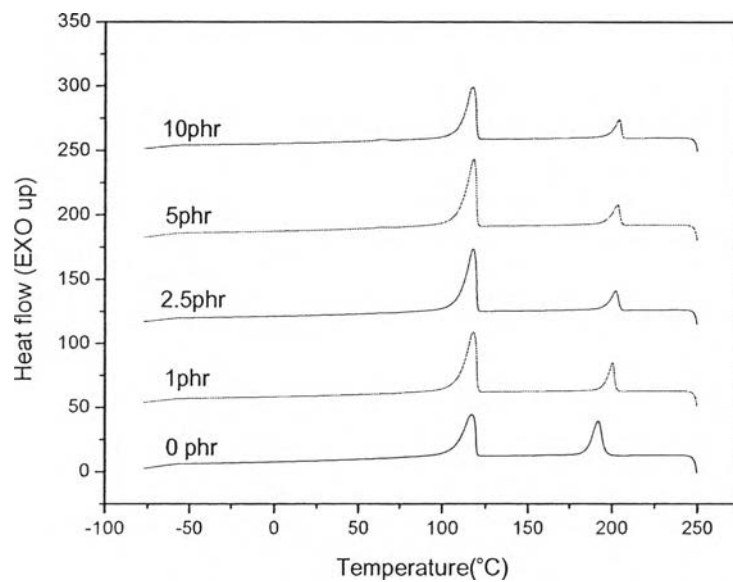
Generally, a single T_g or its shift in blends represents miscibility or partial miscibility. The glass-transition temperature of HDPE was usually not detectable by DSC because of its low amorphous fraction. Although PBT is semi-crystalline polymer, the T_g are not properly observed in Fig.4.21 (b) (which may be attributed to the poor quality of the data exported from the TA Instrument and from the overlay

plotting of these data in the same figure). But in the heating trace, two melting peaks for PBT appeared.

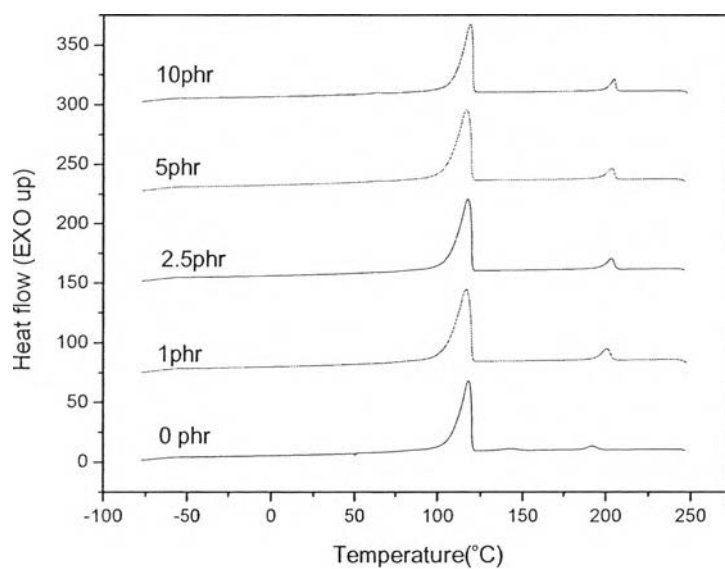
The DSC exotherms obtained at a cooling rate of 10.00 °C/min for the different amounts of Surllyn in the blends of HDPE/PBT 30/70, HDPE/PBT 50/50 and HDPE/PBT 70/30 are shown as figures.



(a)



(b)



(c)

Figure 4.22 DSC melt crystallization exotherms for HDPE/PBT 30/70 blend (a), HDPE/PBT 50/50 blend (b) and HDPE/PBT 70/30 blend (c) samples recorded during cooling at 10 °C/min.

The results suggest that both HDPE and PBT components in the blends crystallized concurrently and that the presence of the more crystallizable HDPE

molecules in the PBT-rich blends helps promote the crystallizability of the blends. As shown in Fig.4.22 (a), the addition of Surlyn shifted the T_c of PBT-rich phase to higher Temperature. The T_c of PBT-rich phase from 0phr to 10phr were 191.7, 200.2, 202.9, 203.1, 204.6 °C, respectively. But the T_c of HDPE phase is nearly keep 116.7 °C, except 10phr increased a little to 117.7 °C.

In Fig.4.22 (b), in HDPE/PBT 50/50 the addition of Surlyn both shifted the T_c of PBT phase and HDPE phase to higher temperature, the T_c variation of PBT phase from 0phr to 10phr was 191.5, 200.3, 202.1, 202.9, 203.9 °C, and the T_c variation of HDPE phase from 0phr to 10phr was 117, 117.5, 117.4, 117.8, 117.1 °C respectively. It could be interpreted as a mutual nucleating agent to enhance the crystallization on the other component.

When the presence of the less crystallizable PBT molecules in the HDPE-rich blends retards the crystallizability of the blends. As shown in Fig.4.22 (c), the addition of Surlyn shifted the T_c of HDPE-rich phase to lower temperature except 10phr. It varied from 117.6, 116.3, 117, 116.4, 118°C respectively. Although the PBT minor phase displayed smaller exothermal peaks, the T_c of PBT phase still shifted to higher temperature.